ORIGINAL ARTICLE

Assessment of recession flow variability and the surficial lithology impact: a case study of Buffalo River catchment, Eastern Cape, South Africa

Solomon Temidayo Owolabi[1] · Kakaba Madi[2] · Ahmed Mukalazi Kalumba[3] · Berhanu Fanta Alemaw[4]

Abstract

The recession identity is an essential indicator of river performance, health and diminution status. This study, therefore, presents an assessment of streamflow recession characteristics in relation to the hydrostratigraphy property of watershed. The streamflow recession assessment was carried out by computing the flow duration curve (FDC) and baseflow index (BFI) analyses of 28 year streamflow records at six distinct streamflow gauging stations. Digital processed aeromagnetic map was hybridized with geological survey and map review for the construction and characterization of concise watershed surficial lithology. The FDC plot of low-flow slopes and Q_{95} reported the flow per station as thus; Buffalo (− 0.0113; 0.0026), Tshoxa (− 0.0029, 0.0016), Yellowwoods (− 0.0022, 0.0008), Mgqakwebe (− 0.0017, 0.0007), Quencwe (− 0.0009, 0.0002), and Ngqokweni (− 0.0005, 0.0001). Similarly, BFI results show the following rank: Buffalo (0.541), Yellowwoods (0.488), Tshoxa (0.450), Mgqakwebe (0.443), Quencwe (0.415), and Ngqokweni (0.332). The recession analysis revealed that the Q_{95} slope of the stochastic FDC approach is a more reliable recession estimate for environmental flow. The assessment of the recession–lithology relationship suggests that the porosity network of the contact zone and fracture system of dolerite may produce a weightier impact of baseflow discharge in support of environmental flow over the hydraulic conductivity of sandstone. The physiographic trends of streamflow response suggest the influence of the high relief on streamflow flux. The overall results suggest that the hybrid approach of FDC and BFI analyses are highly effective for replicating the streamflow recession at the catchment stage and could be adopted for investigation of river sustainability.

Keywords Streamflow response · Flow duration · Baseflow index · Surficial lithology · South Africa

Introduction

The severity of aridity, climate change, and urbanization are a few of the major factors that complicate watershed management, especially in arid environments. Limited knowledge of flow hydrodynamics in the past has brought about the disruption of river health, diminution of streams, lowering of baseflow, distortion of water regime, and a consequential loss of biodiversities (Rivers-Moore et al. 2007; Mirus and Loague 2013). Hence, extensive researches have been carried in recent decades on catchment hydrology owing to the incommutable role of water in environmental sustainability. The researches have, therefore, deepened the understanding of hydro-climatic processes, streamflow dynamics, and hydrologic modeling capabilities essential for catchment and environmental flow management (Brierley and Fryirs 2013). One of the crucial awareness made is the influence of stream hydrodynamics and flow regime on morphogenetic

✉ Solomon Temidayo Owolabi
solomonowolabi11@gmail.com

1 Department of Geology, Faculty of Science and Agriculture, University of Fort Hare, Private Bag X1314, Alice, Eastern Cape 5700, South Africa

2 School of Biological and Environmental Sciences, Faculty of Agriculture and Natural Sciences, University of Mpumalanga, Private X11283, Nelspruit, Mpumalanga 1200, South Africa

3 Department of Geography and Environmental Science, Faculty of Science and Agriculture, University of Fort Hare, Private Bag X1314, Alice, Eastern Cape 5700, South Africa

4 Department of Geology, Faculty of Science, University of Botswana, Gaborone, Botswana

alteration, water balance, groundwater zone budget, and ecological functions (Wella-Hewage et al. 2015). The investigation of the dissimilarities in streamflow patterns and the long-term changes in baseflow within a watershed has enhanced the characterization of hydrologic patterns and river basin management (Esralew and Lewis 2010).

In particular, the knowledge of low-flow and baseflow has contributed to the understanding of shallow subsurface storage processes, hydrologic budget, low-flow dynamics, intrinsic hydraulic properties of the subsurface, and environmental flow condition (Smakhtin 2001; Barlow et al. 2015). To this end, Vogel and Kroll (1992) underpin the relationship between low-flow deductions and the product of average watershed slope, baseflow recession constant and catchment area. Their analysis reveals that the constant of baseflow recession can serve as an important indicator and surrogate for catchment hydraulic conductivity and soil porosity. The study by Chapman (1999) reveals that the streamflow recession can serve as an important estimator. Kienzle (2006) established that the recession index indicates the integral response of catchment in a low rainfall regime, it provides information on the storage capability of a catchment and serves as an indicator for streamflow recovery. A time-series evaluation of the recession rate by Mair and Fares (2011) reported a major slump in baseflow and this was linked with the impact of urbanization. The study by Barros et al. (2017) reveals that the decadal component of baseflow can be used to forecast drought events.

The two major terms associated with recession flow are low-flow and baseflow. Low-flow is the minimum average flow that can be expected in a stream in the dry season or during a hydrologic drought while baseflow is a component of streamflow affected and discharged by shallow subsurface storage (Stuckey 2006; Price 2011). Some of the major natural factors that influence low-flow and baseflow include environmental geology, land use/land cover change, climate change, groundwater aquifer, basin physiography, the geomorphic attribute of the drainage network, soil cover, and local evapotranspiration/evaporation rate (Price 2011). Flow duration curve and baseflow separation are two of the major popular approaches used over time to evaluate the recession rate (Hamel and Fletcher 2014; Gore and Banning 2017; Longobardi and Van Loon 2018; Sarailidis et al. 2019).

Baseflow is basically deduced from the investigation of streamflow time-series hydrographs. Varieties of methods have been proposed for baseflow separation. These include smoothed minimum technique, popularly known as constant-discharge method (Institute of Hydrology 1980), half-linear minimum/maximum technique, popularly referred to as the concave method (Bates and Davies 1988), efficient subsurface flow technique, constant-slope method, Wittenberg technique (Wittenberg 1999), and the master curve method (Cimen and Saplioglu 2004). However, these procedures were improved upon through the development of the automated baseflow separation techniques based on the following approaches, namely, recession curve method, filter-based method, and mass balance method. The recession curve method involves the deduction of recession constant, which can be estimated from the slope of the falling limb of stream hydrograph. The most common recession curve methods include the baseflow index method, hydrograph-separation method, and PART method. The filter-based method is based on signal processing theory. In this method, the low-frequency signal component is separated from the high-frequency signal component. The filter-based method can be further subdivided into two types: recursive digital filter and runoff-stoppage-time method. The recursive digital filter was developed by Eckhardt (2005). The recursive digital filter works by computing the recession analysis and adopting the backward-moving filter in processing quick flow and baseflow attributes (Collischonn and Fan 2013). It is associated with the key assumption of linearity between storage and aquifer water outflux (Zhang et al. 2017). Its estimations are based on discharge record which computes using moving time-window algorithm and basin drainage area only (Lott and Stewart 2013). The mass balance method is carried out using the estimation of the concentration of conservative chemical constituents in the flow components of streamflow, such as hydrogen or oxygen isotope ratios (Stewart et al. 2010). It involves concurrent sampling of streamflow rate and chemical concentrations. This is, however, laborious and expensive while extreme caution is required on the choice and composition of isotopic tracers as well as the procedure of experimentation to be followed for accurate results (Lott and Stewart 2013).

Flow duration curve (FDC) is the plot of the observed historical variation of flow with the percentage of time resolution to show the percent of time specified discharges were equaled or exceeded over a given period (Verma et al. 2017). It involves the computation of the cumulative frequency curve of flow at a defined time domain (Searcy 1959). The time resolution can be prepared as mean daily, weekly, monthly or seasonal discharge. The shape of the curve can be used to deduce information on the regime property of the river in the high flow, and the sustenance of the river in the low-flow. In general, it provides information on the flux of streamflow and storage capability of the catchment (Müller et al. 2014). Many methods have been proposed for computation of FDC, and these can be classified into three based on the computational approaches: (a) statistical approaches, (b) graphical approaches, (c) and parametric approaches (Castellarin et al. 2004; Requena et al. 2018). Of the approaches, the most widely used FDC procedure especially for estimation of low-flow is the statistical approach, which is based on probability distribution function (Gustard and Demuth 2009). Fennessey and Vogel

(1990) estimated the receding low-flow section of daily FDC with the aid of two-parameter log-normal probability density functions to develop a regional hydrologic model. Jha et al. (2008) presented the applicability of probability density-based FDC for modeling relationship between the frequency and magnitude of environmental flow. Basso and Botter (2012) developed an analytical expression for investigating the optimal streamflow energy production and economic management of hydropower plant using probabilistic FDC and minimum environmental flow requirement. Booker and Woods (2014) noted that flow duration curves estimated from empirically based machine learning regression model serves as an important tool for correcting the uncalibrated physically based rainfall-runoff model. Verma et al. (2017) demonstrated the smoothness and effectiveness of 7D-MA among other scenarios of moving averages for the computation of Period-Of-Record FDC (PORFDC), and 10- and 100-return year of 95% equaled-or-exceeded (Q_{95}) of stochastic FDC (SFDC) assessment. Requena et al. (2018) proposed the estimation of FDC using functional multiple regression owing to its flexible framework, its robustness with larger percentage of sites, and its analytical insights on descriptors. Burgan and Aksoy (2018, 2020) presented a probability distribution function-based FDC model computed by nondimensional normalization of annual mean streamflow data series. Computation also incorporates drainage area and precipitation in its empirical regression model. The simplicity, robustness and analytic insights of statistical FDC for investigation of environmental flow, especially the receding low-flow, accounted for its recommendation by World Meteorological Organisation for eco-flow analysis (Gustard and Demuth 2009). However, the entwined assessment of low-flow together with baseflow index for corroboration or veritability purpose is quite uncommon in the literature.

Despite the significance of baseflow in recession flow, studies involving the comparative study of the hydrostratigraphic influence on recession flow are rare as noted by Barthel (2014), Barthel and Banzhaf (2016), Haaf and Barthel (2018), and Carlier et al. (2018). Based on the bibliometric assessment of publications from January 1990 to November 2019 in Web of Science portal, very few studies were carried out on the streamflow–lithology relationship. Among these are Ward and Robinson (1990) and Mayer and Naman (2011), that noted that acknowledge the significant impact of geologic parameters on the shapes of FDC and streamflow response to climate change. Nippgen et al. (2011) and Naef et al. (2015) also reported the significance of sandstone on account of its hydraulic conductivity to streamflow as it buffers its mean transit time during the dry periods. Carlier et al. (2018) indicated that the bedrock and its permeable quaternary deposit component have a weightier influence on catchment hydrology than other catchment characteristics.

The studies with more critical analyses of bedrock relationships with streamflow attributes are Pfister et al. (2017) and Sanz and Atienzar (2018). Pfister et al. (2017) compared bedrock characteristics to precipitation–discharge ratio, catchment storage deficit (based on catchment water balance computation), and catchment hydraulic turnover (based on isotopic signal damping). The study highlighted that the hydraulic conductivity of bedrock is the main intrinsic property controlling groundwater system interaction with streamflow recession processes. However, the approach is parameter-driven, robust, and complex, especially in the data-scarce environment. Sanz and Atienzar (2018) developed an approach for quantifying the river performance, based on groundwater storage capacity. The development of the approach (referred to as LIT) was based on the strong correlation which exists between the classes of river basin rock types (in terms of aquifer capacity) and the computed environmental flow relative to river basins.

The approach engaged in this present paper specifically focuses on spatial variability in recession flow pattern within a watershed and the contribution of hydrogeologic characteristics to the pattern. The work intends to address the knowledge gap on the relationship between low-flow attributes to baseflow components in recession flow assessment. It intends to present the technical feasibility of delimiting regional geological information into locally distinct boundaries of surficial lithological for catchment-scale studies. And lastly, it intends to unravel the critical ramifications associated with a holistic assessment of streamflow–lithology characterization. The novelty of this present paper lies in the regional context. No previous study on streamflow modeling has been carried out in the study area. In the regional context, Xu et al. (2002) presented geomorphological stages of streams in South Africa, which were classified as upper, middle and lower courses and then related to hydrogeological settings for baseflow discharge estimation. In a similar manner, Vegter and Pitman (2003) carried out a regime-based hydrologic assessment of streams in South Africa, which classified streams into ephemeral, seasonal and perennial. The work identified two types of disconnected streams: the detached (based on the imperviousness of its surficial lithology) and famished stream (based on exceedance of evaporation rate to recharge rate) (Vegter and Pitman 2003). Van Wyk et al. (2012) established through the hyetograph–hydrograph time-series dataset that there is evidence of the time-bound infiltration phase during early summer rainfall, while groundwater recharge/discharge potential depends on the status and field capacity of the unsaturated zone reservoir.

Hence, the aim of this study is to characterize streamflow hydrodynamics recession properties of Buffalo watershed in relation to hydrostratigraphic properties of the watershed. The examination of recession flow is based on the rationale

that the diminution potential of the river depends on the weakness of low-flow and baseflow index, which is primarily influenced by the hydrostratigraphic units. Moreover, recent studies on streamflow variabilities and stormwater management emphasize the necessity for catchment-based hydrologic assessment (Wella-Hewage et al. 2015). As a consequence, the following research questions were addressed:

1. What are the actual recession flow characteristics of the watershed and which method of stream recession assessment is the most suitable at the catchment scale?
2. How does the streamflow recession vary with the lithologic heterogeneity of the catchment?
3. What can be inferred from the relationship between streamflow recession and the groundwater level?

The catchment-based hydrologic assessment is accomplished by addressing the following objectives: (1) by quantifying the low-flow and baseflow index variability across sub-catchments; (2) by reconstructing the local surficial lithostratigraphic pattern through regional geology map review, geologic survey, digital processing of aeromagnetic map; (3) by inferring the influence of surficial lithology property on the streamflow recession characteristics; (4) by corroborating the inter-relationship between recession flow variability and groundwater level. The paper presents a comparative assessment of the recession flow of the Q_{95} of the 7D-MA approach of PORFDC and SFDC alongside the average baseflow index estimate for environmental flow assessment. It also presents the hybridization of secondary geology map with geologic survey and digitally processed aeromagnetic map for characterization of watershed environmental geology. The assessments report the vulnerability potential of the watershed mini-rivers to hydrologic drought. It is considered that the study approach would be beneficial to the policymakers, water stakeholders and engineers.

Study area

The study area is situated in the headwater of the Buffalo catchment, Eastern Cape Province, South Africa. It lies between latitude S32° 40′ and S32° 59′ (36 km long) and longitude E27° 00′ and E27° 33′ (41 km wide), covering an approximated area of 1237 km^2 (Fig. 1).

It is drained by the Buffalo River, which runs Southeastward towards the Indian Ocean. The river stretches across an approximated length of 126 km. The study area landform is characterized by three main terrain types: the medium gradient mountain in the Northwest, the dissected plain which flanks from the West to the Northeast and East, and the plain which spreads across the Southwest, South, and Southeast (Bailey et al. 2011). The relief of the area has a range of 258–1370 m above mean sea level. The hydrologic periods run across four seasons from October to September: spring (September–November), summer (December–February), autumn (March–May), and winter (June–August).

The mean annual rainfall from the central station at Bhisho is estimated to be 590 (mm/year) for 1989–2016.

Fig. 1 Buffalo River Catchment map showing the drainage system
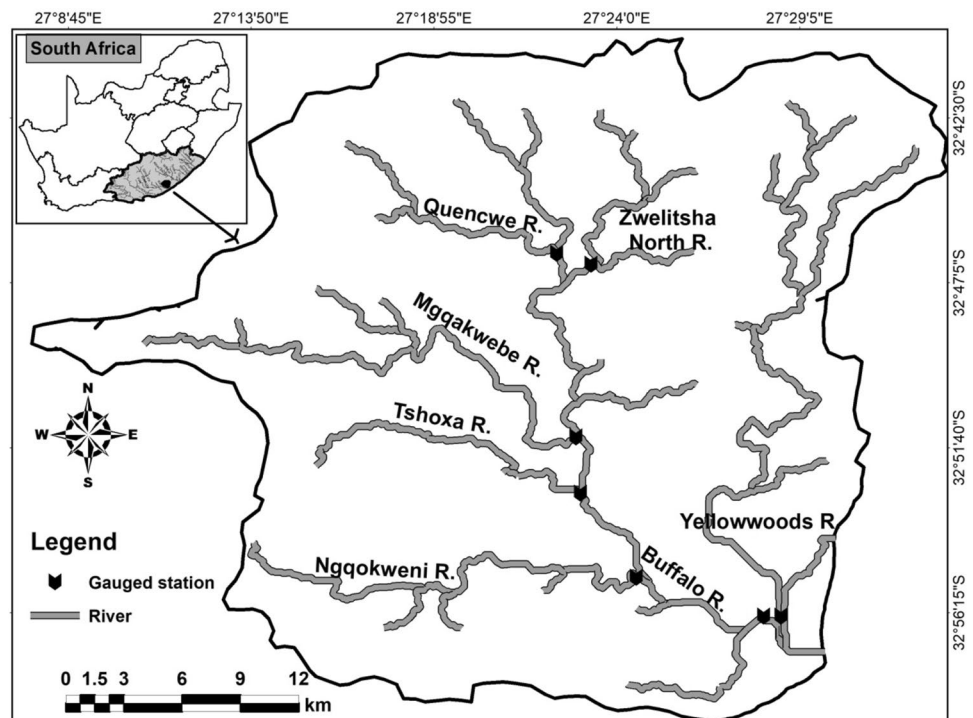
Rainfall varies from the hilly terrain and natural forest to the plain in the Northwestern to Southeastern direction. The average minimum temperature is 13.5 °C in general, and as low as − 3 °C in winter at the hilltop (Slaughter et al. 2014). The average maximum temperature is 22.3 °C across the environment, while the maximum summer temperature is 38 °C at the plain especially at Gwaba (Slaughter et al. 2014). Buffalo River is supported by six reaches: Ngqokweni, Tshoxa, Mgqakwebe, Quencwe, Zwelitsha North, and Yellowwoods Rivers (Bailey et al. 2011). The section of Buffalo River catchment captured within the study area terminates at the river mouth to the Laing Dam, approximately 54 km in length. Other necessary physiographic information that is relative to the drainage boundary encapsulating the streamflow gauging stations are presented in Table 1.

The major section of the catchment basin is underlain by Permian–Triassic arenaceous mudstones of Balfour formation while the Southern minor segment of the catchment is underlain by Permiam argillaceous shaly-sandstone of Middleton Formation (Baiyegunhi 2015). There are outcrops of Jurassic dolerite intrusion at distal points across the hydrologic basin (Oghenekome et al. 2016). Catuneanu and Elango (2001) established that the biostratigraphic record of the paleoenvironment indicates paleoclimate which is humid-to-temperate with no evidence of climate change. Oghenekome et al. (2016) also noted that the general morphology of grain sizes of the formation reveals evidence of chemical and depositional immaturity. This suggests that the paleoenvironment is a low-energy environment with respect to climatic fluctuation. The formation belongs to the Adelaide Subgroup, of Beaufort Group, within Karoo Supergroup (Table 2; Johnson 1976; Wilson et al. 2014). The semi-arid area is characterized by fractured rock aquifer type (Vegter and Pitman 2003).

Materials and methods

Six gauging stations were identified within the hydrologic basin headwater: Ngqokweni, Tshoxa, Mgqakwebe, Quencwe, Buffalo, and Yellowwoods stations. Hence, their

daily streamflow data from 1956 to 2017 were acquired from the Department of Water Affairs and rainfall data was acquired from South Africa Weather Service. The data were inspected for missing records and consequently reduced to 28 years records which spanned from January 1, 1989 to December 31, 2016. This just agrees with the minimum of 25 years of data series requirement for average statistical assessment for trends and variability study in Burn and Elnur's (2002) work. Within the 28 years' record, missing data were less than 0.01%. The missing days were extrapolated by taking the average of the preceding 2 days and the succeeding 2 days. All the data were summed into monthly and seasonal records. Prior to the computation of the streamflow recession information, the descriptive statistics of the processed streamflow dataset was examined.

Quantification of streamflow recession attributes

Flow duration curve computations

The streamflow may be discretized as daily, weekly, monthly or yearly intervals. In this work, flow frequency is discretized 7-day moving average (MA). Two major assessments were computed as outlined below;

1. Period-of-record FDC
2. Stochastic FDC

Period-of-record FDC

Period-of-record (POR) FDC was carried out by computing the cumulative density function of monthly scenarios in a strategic manner. In this work, the cumulative density function was computed using a 7-day moving average. The computation was achieved through the following steps;

1. Columns were prepared in a spreadsheet for a 7-day moving average for each of the sub-catchments.
2. The moving averages were sorted in descending order.
3. Time step interval was created, using the rank of numbers for q_i, where $i = 1, 2, 3,\ldots,n$, for which n is the total number of periods of record across the time series,

Table 1 Important characteristics of streamflow gauging stations in Buffalo catchment

S/N	Stations	Sub-basin area (km²)	Relief, R (m)	Basin length, L (km)	Relief ratio (R/L)	Mean annual runoff (cumec)
1	Buffalo	668	1112	42.97	25.88	433.89
2	Yellowwoods	198.4	670	36.50	18.36	169.07
3	Ngqokweni	103	285	23.74	16.70	73.52
4	Quencwe	61	943	19.36	48.71	79.22
5	Mgqakwebe	119	914	29.34	31.15	131.77
6	Tshoxa	411	280	16.77	16.70	405.36

Table 2 Lithostratigraphy of the regional geology of the site (Johnson et al. 2006)

Supergroup (subgroup)	Subgroup	Formation	(member)	Lithology	Depth (m)	Epoch	(period)
				Alluvium, Dunes and beach sands	Varies	Holocene (Recent)	
(KAROO (Beaufort)	TARKASTAD	Burgersdorp		Red Mudstone Sandstone Light Grey Sandstone Grey Shale	1000	Triassic	(Anisian)
		Katberg		Light Grey Sandstone Red Mudstone Grey Shale	900		(Scythian)
	ADELAIDE	Balfour	(Palingkloof)	Red Mudstone Light Grey Sandstone	50	Permian	(Tatarian)
			(Elandsberg)	Sandstone Siltstone	700		
			(Barberskrans)	Light Grey Sandstone Khaki Shale	100		
			(Daggaboersnek)	Grey Shale Sandstone Siltstone	1200		
			(Oudeberg)	Light Grey Sandstone Khaki Shale	100		
				Grey and Black shale			(Kazarian)
		Middleton		Light Grey Sandstone Red Mudstone	1500		
		Koonap		Grey Sandstone Shale	1300		(Ufimiam)

while m is the rank of annual extreme series arranged in descending order of magnitude.

4. Weibull plotting formulae (Eq. 1) was employed to compute the corresponding probability, P, of exceeding individual flow, i, from the rank.

$$p = \frac{m}{n+1} \times 100, \tag{1}$$

$$P = P(Q > q_i) = 1 - P(Q \le q_i). \tag{2}$$

5. The plot of flow (for each of the sub-catchment) against the corresponding probability, P, (from Eq. 2) is presented in a log-normal graph. P is drawn on the x-axis against the magnitude of a 7-D moving average of the stream discharge on the y-axis.

80th to 99th percentile (Q_{80}–Q_{99}) was assessed for low-flow across each sub-station. Plots of PORFDC were analyzed for the information on the variability of low-flow relative to environmental flow sustenance (Ye et al. 2018). The recession pattern of the curve provides information on the characteristics of the terrain and stream channel (Croker et al. 2003).

Stochastic FDC

Stochastic FDC was computed by disaggregating streamflow daily order into an individual annual record and plotting the cumulative density function in relation to a specific order of the FDC plot. Seven-day moving average order was adopted owing to its smoothness among others as obtained from the PORFDC. The computation was achieved through the following steps outlined below:

1. Annual FDC plots were produced for the six stations using the steps outlined in the preceding section.
2. Each 5% probability of exceedance was marked, while, only the 95th percentile (Q_{95}) of the FDC was extracted across the annual columns of aggregates.
3. The extracted Q_{95} values were sorted in ascending order and assigned ranking order; using $i = 1, 2, 3, \ldots, n$ for ranking order.
4. Probability of exceedance, P (Eq. 2), was deduced from the rank value using Weibull formulae (Eq. 1).
5. The deduced Stochastic FDC probability of exceedance, P, was plotted against the sorted Q_{95} characteristics using a trend-line for the derivation of the equation of a best-fit line.

The slope of the Q_{95} AFDC Plot was assessed for low-flow variability while R2 suggests the degree of disturbance influencing the trend of the low-flow. The temporal consistency in low-flow dynamics with respect to governing environmental conditions is therefore revealed by the FDC plots (Verma et al. 2017).

The procedure for baseflow separation

Due to uncertainties that might be associated with the use of one baseflow separation procedure and the rigor of validating the deductions, five different approaches were employed. Their average value was taken and adopted. Hence, 28 years of streamflow data set, from 01 Jan 1989 to 31 December 2016, was analyzed using two-parameter digital filter program (TwoPDF), PART program, hydrograph-separation (HYSEP) local minima program, standard baseflow index (BFI) program, and BFI modified program within USGS groundwater toolbox package.

The BFI standard computation partitioned the streamflow records into intervals (N) of 5 days. The minimum streamflow value for each of the intervals was compared to the minimum streamflow value of its adjacent partition interval to deduce its turning point. The result was also tested using a turning point test factor of 0.9, such that if 90% of a specific minimum is less than the preceding and the following adjacent minimums, then the specific minimum is a turning point. The turning points were then connected to generate the baseflow hydrograph (Wahl and Wahl 1995). The major difference in the computation of BFI standard and BFI modified is the use of recession constant (K') in place of the turning point test factor (f) according to the following equation by Barlow et al. (2015):

$$K' = f^{\left(\frac{1}{N}\right)}, \tag{3}$$

where the values of $f = 0.9$, and $N = 5$. Hence, $K' = 0.97915$. More information on the Standard and modified baseflow index are provided by Wahl and Wahl (1995).

Baseflow computation based on the two-parameter digital filter (TwoPRDF) approach was carried out using the low-pass filter algorithm Eq. (4) (Eckhardt 2005):

The filter was passed over streamflow record once in order to smoothen the baseflow hydrograph (Arnold et al. 2000; Barlow et al. 2015), while BFImax was modeled by the algorithm. The TwoPRDF configuration is based on the assumption that the addition of baseflow and streamflow equals the total streamflow, and that the relationship between aquifer storage and baseflow [into stream] is a direct variation. The default value for the baseflow filter parameter was used ($\alpha = 0.98$) to ensure a uniform baseflow extraction condition for the six stations that were assessed. More information on this method is provided in detail in Eckhardt (2005).

The PART program is based on the streamflow partitioning principle. It equalizes baseflow for streamflow on days that are assigned as being unaffected by interflow. This is based on the antecedent streamflow recession, given that other components of the flow, such as evapotranspiration, are negligible. Meanwhile, the remaining parts of the hydrographs are linearly interpolated. The days that are not affected by run-off (N days) are indicated by the continuous recession (Barlow et al. 2015). Its response time is expressed in terms of the drainage area, A (1237 km^2) as shown in the following equation:

$$N = A^{0.2}. \tag{5}$$

The daily values of baseflow were obtained by searching the arrays of streamflow for days that fit the antecedent recession requirement three times for three different values of N. The final result of baseflow for each day was estimated from curvilinear interpolation of the three different values of N. More information on the algorithm of the PART program is documented in Rutledge (1998). This program is run three times for each streamflow for consistency reasons.

The HYSEP program was developed by Pettyjohn and Hennings (1979). It computes in a similar way to the PART program using an algorithm of the relationship between basin drainage area (A) and duration (N days) of the recession limb of the hydrograph (Eq. 5). There are three types of HYSEP programs: fixed block, sliding block and local minimum method. Each of the methods estimates baseflow with unique algorithms. The HYSEP fixed block approach computes baseflow by searching the hydrograph for minimum streamflow at an interval of 2 N days from the first day of streamflow record. The HYSEP sliding block approach

$$B_{k+1} = \frac{\left(1 - BFI_{max}\right) \times \alpha \times B_k + (1 - \alpha) \times BFI_{max} \times Q_{k+1}}{(1 - \alpha) \times BFI_{max}} \quad \text{if } B_{k+1} \leq Q_{k+1}, \tag{4}$$

where BFI_{max} is maximum baseflow index, the ratio of baseflow to streamflow, $\alpha =$ baseflow filter parameter, $Q_{k+1} =$ streamflow at time step $k + 1$, $B_k =$ baseflow at time step k.

computes baseflow by default searching for the minimum streamflow within an interval of 2 N days between day-3 and day-11. The HYSEP sliding block approach allows the designation of the day of interest where the baseflow computation

can begin. The major difference between the previous two methods and the HYSEP local minima method is the fact that the local minima method checks each day within the hydrograph interval to ascertain if the minimum streamflow is the lowest within $0.5(2N-1)$ days before and after the day. If the check is true, then it is considered the local minimum, while the turning points are joined by linear interpolation (Rudra et al. 2010). In this work, the local minimum method was employed due to the further process of checking for the local minimum which also further reduces uncertainty. This method began its estimation by building a sequence of local minima for each day recorded with the lowest flow within intervals of days with sequential runoff or recession. For further information on HYSEP, see Barlow et al. (2015).

The results of daily baseflow, daily runoff, and baseflow index were generated for each of the methods. The baseflow index results for each of the five baseflow methods used were extracted and computed to monthly mean across the hydrologic year. This was done to simplify the comparative analysis of the results. The results were projected as a baseflow index (BFI) plot. The plot provides information on the water storage–discharge attributes of an aquifer that can be linked with aquifer's intrinsic properties such as transmissivity, porosity, permeability, and hydraulic gradient (Barlow and Leake 2012). The BFI results were compared to the low-flow and recession plots of FDC.

Conceptualization of the surficial lithology and its influence on the river basins

Due to the significance of lithologic control on streamflow, a local geological survey of the area was done through the review of regional geology maps, digital processing of aeromagnetic data and field survey. Identification of boundaries of bedrocks during the digital processing of the aeromagnetic data was supported by field geology mapping and cross-section profiling of lithologic information of 576 borehole data drilled within the watershed from 1952 till 2014. The aeromagnetic map extracted for the study area was acquired from Fugro Airborne Surveys. The aeromagnetic survey was done using a proton precession magnetometer of 0.01 nT resolution, while its flight was done at a constant height of 60 m in North–South flight direction, within the sampling line of 250 m at a line spacing of 200 m. The extracted magnetic data were processed using the filtering algorithm of the Montaj MAGMAP filtering system. First, the data were "reduced to pole" by removing the International Geomagnetic Reference Field using the average magnetic inclination and declination of $63.47°$ and $-28.67°$, respectively (Figure A; Peddie 1982). The "reduction to the pole" operation re-computes the total magnetic intensity data as if the inducing magnetic field is inclined and declined by the value used. Convolution

and data filtering in the wavenumber domain using two-dimensional forward and inverse fast Fourier transform (FFT) algorithms were carried out prior to calculation of the analytical signal and projection of the geologic map.

The field geology mapping exercise involved the delineation of boundaries of surface detrital and sedimentary facies for ground-truthing purposes. The borehole lithologic data were downloaded from the national groundwater archive of South Africa. The result of the field mapping and lithology cross-section profiling was used as a guide for supervised mapping of the tone amplitude classification resulting from analytical signal calculation. The maximum likelihood approach was used while the surficial lithology was classified into three dominant rock sections: dolerite, mudstone and sandstone sections, as obtained from the field geology mapping and lithology cross-section.

Corroboration of streamflow findings with aquifer properties

To accomplish the second objective, the variability in groundwater level and borehole yield across the sub-catchments was explored. Data sets for water level and borehole yield were downloaded from the national groundwater archive of South Africa, http://www3.dwa.gov.za. 160 borehole yield data and 400 water levels were used and classified according to their sub-basins. Each class was represented on a box-and-whisker plot by computing for their minimum value, lower quartile, median, upper quartile, and maximum value. These were used to derive the estimate for the bottom, 2Q box, 3Q box, whisker– and whisker+ (Table 3; Krzywinski and Altman 2014). The relationship between the plots and the information projected from the streamflow recession were compared.

Results

Statistical summary of streamflow data

Table 4 reports the summary of the streamflow descriptive statistics for each station in the watershed. The report shows the variability in streamflow response to

Table 3 Box-and-whisker plots parameters

Box-parameter	Formula
Bottom	Lower quartile
2Q Box	Median–lower quartile
3Q Box	Upper quartile–median
Whisker–	Lower quartile–minimum value
Whisker+	Maximum value–upper quartile

Table 4 Statistical summary of the streamflow data from 1989 to 2016

Stations	Range (cumec)	Min (cumec)	Max (cumec)	Mean (cumec)	SD (cumec)	Variance (cumec)	Skewness	Kurtosis
Buffalo	291.93	2.64	294.56	36.16	43.69	1908.99	2.47	7.97
Yellowwoods	210.26	0.05	210.31	14.09	27.97	782.18	3.75	16.86
Ngqokweni	68.10	0.04	68.13	6.20	11.92	142.19	3.22	11.14
Quencwe	129.44	0.14	129.58	6.51	12.62	159.16	5.09	37.32
Mgqakwebe	138.85	0.08	138.93	10.83	18.43	339.54	3.48	15.68
Tshoxa	592.10	0.04	592.14	33.08	63.12	3983.66	4.32	26.97

hydro-climatic, geomorphic and aquifer influences on the sub-drainages.

The highest flow, deviation, and variance skewness occur in Tshoxa station while the least occurs in Ngqokweni station. Although Tshoxa station is smaller in size to Ngqokweni, its descriptive statistics suggest that Tshoxa flow may have been favorably influenced by a higher proportion of baseflow discharge. This accounts for higher streamflow proportion in the station compared to the flow in other sub-catchments. The result of kurtosis and skewness indicate the extremity of temporal variability in the statistics of Quencwe station among others. The reports suggest that the streamflow in high relief has the tendency not to be normally distributed due to its turbulent nature, which is influenced by the hillslope factor. Buffalo flow is the major stream order for most of the stations except Yellowwoods station, hence, this may account for its higher mean discharge than others. Here, the order of response to climate variability and environmental factors, corresponding to standard deviation and variance, from the highest to the least, are Tshoxa, Buffalo, Yellowwoods, Mgqakwebe, Quencwe, and Ngqokweni flow.

Low-flow assessment

The low-flow section of the FDC provides information on the extent of groundwater discharge to support

environmental flow in the dry season. The result as indicated on the PORFDC plot for the low-flow region (90th to 99th percentile time exceeded) in the order of decreasing recession are presented as thus (Fig. 2); Buffalo (− 0.0113), Tshoxa (− 0.0029), Yellowwoods (− 0.0022), Mgqakwebe (− 0.0017), Quencwe (− 0.0009), and Ngqokweni (− 0.00049). The plots of Q_{95} for AFDC of the six stations are presented in Fig. 3.

The results further confirm the deductions made by the low-flow plots. The AFDC plot of Mgqakwebe, Buffalo and Ngqokweni showed the strongest consistency in low-flow trend compared to Quencwe station which showed the least consistency based on the coefficient of confidence (R^2). The R^2 revealed that hydrologic alterations across all the streamflow are minimal and that the low-flow plots represent the actual field condition meanwhile the alteration is higher in Quencwe River than others. The R^2 aligns with the deduction of kurtosis (Table 3).

The low-flow results, therefore, indicate that groundwater discharge to support streamflow is higher at Buffalo station than other stations. This may be consequential to its stage, as the last stream order for the watershed was where accumulated flow occurs. The trend of decline in the low-flow recession at Tshoxa to Ngqokweni station indicates the possible order of baseflow contribution to streamflow across the watershed. The low-flow assessment suggests that groundwater discharge to Tshoxa River

Fig. 2 FDC plot of 1989–2016 streamflow records across the six stations in Buffalo catchment
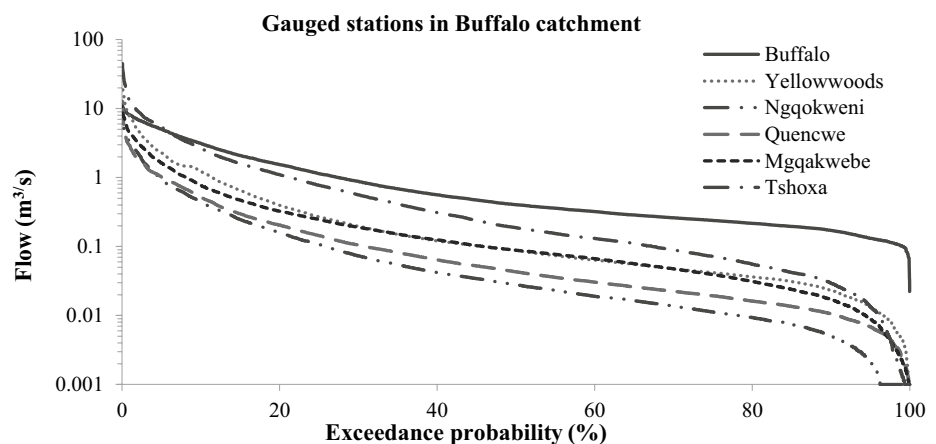
Fig. 3 Low FDC plot using Q95 across the AFDC from 1989 to 2016 for; **a** Buffalo, **b** Yellowwoods, **c** Ngqokweni, **d** Quencwe, **e** Mgqakwebe, and **f** Tshoxa stations

A   Buffalo R.

$y = 0.0026x + 0.07$
$R^2 = 0.9362$

B   Yellowwoods R.

$y = 0.0008x - 0.0039$
$R^2 = 0.8715$

C   Ngqokweni R.

$y = 0.0001x - 0.0011$
$R^2 = 0.9123$

D   Quencwe R.

$y = 0.0002x - 0.0006$
$R^2 = 0.851$

E   Mgqakwebe R.

$y = 0.0007x - 0.0077$
$R^2 = 0.9457$

F   Tshoxa R.

$y = 0.0016x - 0.0249$
$R^2 = 0.8655$
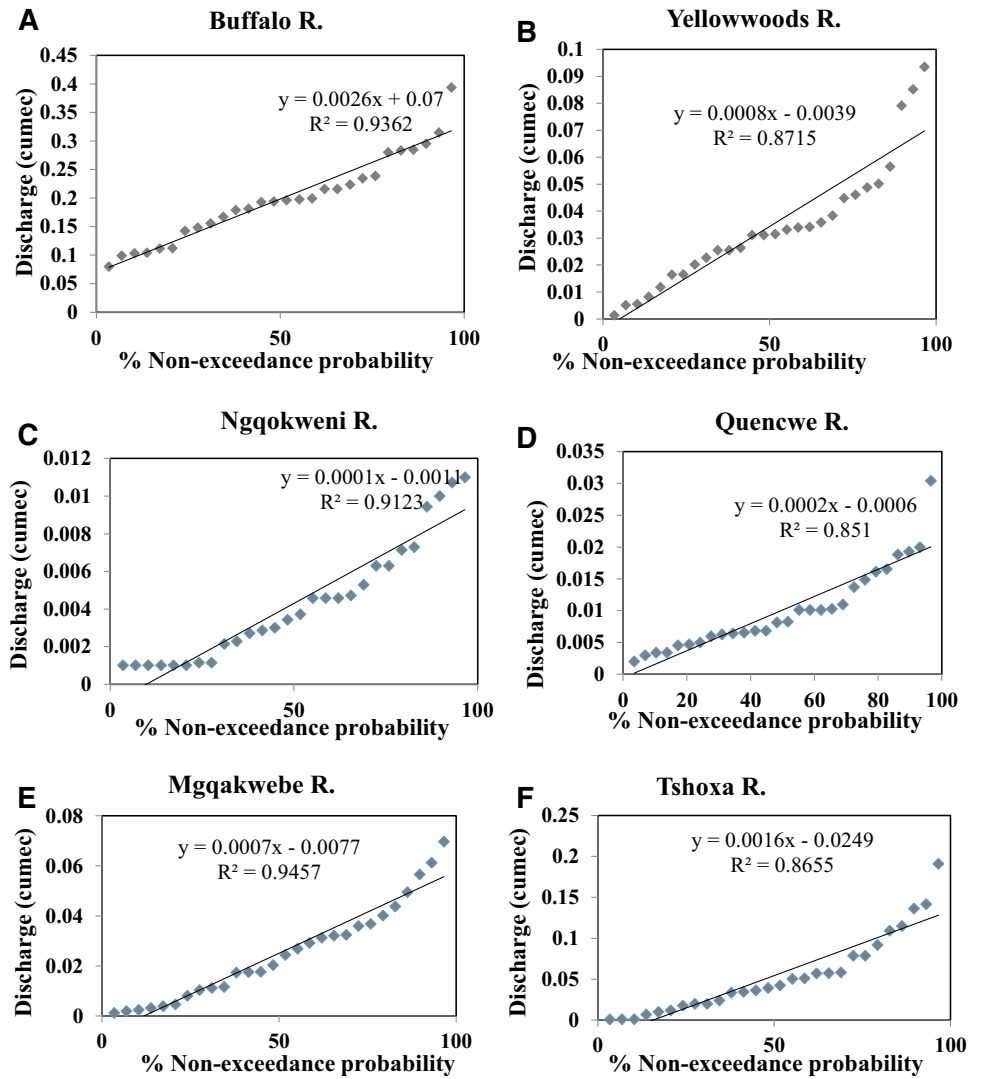
dry season is higher compared to others. It also indicates that the Ngqokweni River is highly vulnerable to hydrologic drought. In other words, the result reports the possible order of connection of the river to the section of the groundwater system where the hydraulic head is higher or the groundwater flow is high due to the hydraulic conductivity of the aquifer material.

Baseflow separation

Results of the mean annual baseflow separation are presented in Table 5. Two-parameter digital filter (TwoPDF) approach provides the reading with the highest estimation, while the baseflow index modified (BFI modified) approach

Table 5 Long-term average annual baseflow for streamflow of 1977 to 2016

Station	Two-PRDF	PART	HySEP-Loc Min	BFI standard	BFI modified	Average baseflow
Buffalo	0.596	0.599	0.525	0.492	0.491	0.541
Yellowwoods	0.551	0.551	0.487	0.426	0.426	0.488
Ngqokweni	0.460	0.432	0.327	0.218	0.217	0.332
Quencwe	0.502	0.484	0.448	0.318	0.321	0.415
Mgqakwebe	0.529	0.515	0.450	0.361	0.358	0.443
Tshoxa	0.541	0.512	0.460	0.369	0.368	0.450

provided the lowest estimation. However, the gap in estimation is controlled by taking the average of the estimations.

Plots of monthly variation of BFI are presented in Fig. 4a–f. From the plots, streamflow composing of the baseflow index of 0.5 or greater (BFI ≥ 0.5) implies that the streamflow is dominated by 50% and more of baseflow discharges.

Hence, the information on the BFI ≥ 0.5 significantly highlights the streamflow with viability for environmental flow sustenance through the dry season of the hydrologic regime. Figure 4a–f reports that the months of dominant baseflow discharge across the watershed begins in June through August. The increase in run-off proportion in the spring suggests that the month of significant hydrologic inception marked by heavy rainfall event is October. The R^2 reveals that there is no significant increase across the hydrologic period due to the oscillatory pattern of regime variability.

Specifically, Buffalo station has the highest baseflow discharge across the hydrologic period (Fig. 4a). The discharge is dominant from February (BFI = 0.532) through October (BFI = 0.626). The station reported the maximum relative baseflow discharge in the watershed in June (BFI = 0.823). The result suggests that the watershed is heavily sustained by baseflow across the hydrologic period. The dominant baseflow discharge in Yellowwoods station occurs in April (BFI = 0.513) through October (BFI = 0.543). For Mgqakwebe flow, it occurs in April (BFI = 0.503) through September (BFI = 0.521). For Tshoxa flow, it occurs in May (BFI = 0.721) to September (BFI = 0.637). For Quencwe flow, it occurs in April (BFI = 0.500) through August (BFI = 0.555). Meanwhile for the Ngqokweni flow it occurs in May (BFI = 0.621) and June (BFI = 0.561).

The results report Ngqokweni as having the least baseflow discharge. It also indicates that Ngqokweni drainage is highly vulnerable to drought owing to the few months of baseflow discharge. The BFI results also indicate Yellowwoods as having a sustainable streamflow structure owing to the extent of baseflow discharge across the hydrologic period. The slope of BFI plots indicates that only Yellowwoods, Tshoxa, and Buffalo are associated with incremental trends, while the slope of Mgqakwebe, Ngqokweni and Quencwe stations are associated with the declining trend across the year. The only spatial pattern in the BFI result points to the influence of the Waterhead. Every other sub-basin except Ngqokweni has its Waterhead lying in the high altitude. This is assumed to influence the quantity of run-off that runs across the river valley. However, the BFI estimate is majorly controlled by the hydraulic conductivity of the hydrologic basin subsurface layer and the existence of geologic structures.

Conceptualization of surficial lithological influence on baseflow and low-flow properties

The reduction-to-pole map, presented in Fig. 5, shows the areas of high and low magnetic anomaly corresponding to important geological conditions in Buffalo subsurface. The analysis reveals the zone of high magnetic anomaly, which is possibly associated with the regions of the deep-seated dolerite plutons. On the field, the regions constitute a contact zone, associated with a fracture system, possibly resulting from the transmission of stress from the hotspot of dolerite. The low magnetic anomaly indicates the lineament features where the pressure of deep-seated magnetic anomaly is probably very low. Overlay of the area by doleritic features of geology map revealed that most of the low magnetic lineaments are covered by dolerite outcrops.

The analytic signal map, presented in Fig. 6, showed the area of a high magnetic anomaly (β_H) coinciding with the area covered by the dolerite outcrops. Lithology cross-section analysis revealed that the area associated with low magnetic anomaly (β_L) is dominated by sandstone while the area covered by $1000 \leq \beta \leq 2500$ nT is dominated by mudstone. This is possibly due to the existence of paramagnetic materials (clay mineral content) in the interstitial pore spaces of sandstone and mudstone (Liu et al. 2017).

The overlay of the resulting geologic survey and the drainage of Buffalo catchment is presented in Fig. 7, while the summary of the distribution of the dominant rocks within the sub-basins is presented in Fig. 8. The surficial lithostratigraphic layer of Buffalo catchment is dominated by fractured arenaceous mudstone strata of Balfour formation. The mudstone component covers an area of 505.47 km^2, ranging from the thickness of 4–45 m at various points across the catchment. The sandstone component covers about 197.63 km^2 thickness and ranges from few centimeters to 90 m thickness of a borehole section in the Tshoxa basin. The dolerite component covers about 266.22 km^2, with extensive weathered sections dominating the outcrops at the West, Northwest, and Northeast. The pervasiveness of the fracture system on and around basement rocks suggests the existence of transmissive zones, developed at the dolerite-sedimentary rock contact zone. This may thereby enhance the development of secondary porosity and further enhance baseflow discharge from the aquifer. Other rock types observed in the field include the shale, siltstone, sandy–siltstone, sandy–shale and intercalated mudrock and sandstones. These were all mapped as interbedded rocks and these cover about 268.68 km^2.

The high baseflow index and favorable low-flow in the Tshoxa basin can be associated with the favorable groundwater discharge from the local aquifer of the Buffalo on account

Fig. 4 Mean annual BFI plots for; **a** Buffalo, **b** Yellowwoods, **c** Ngqokweni, **d** Quencwe, **e** Mgqakwebe, and **f** Tshoxa stations

Fig. 4 (continued)

Mgqakwebe River

Tshoxa River
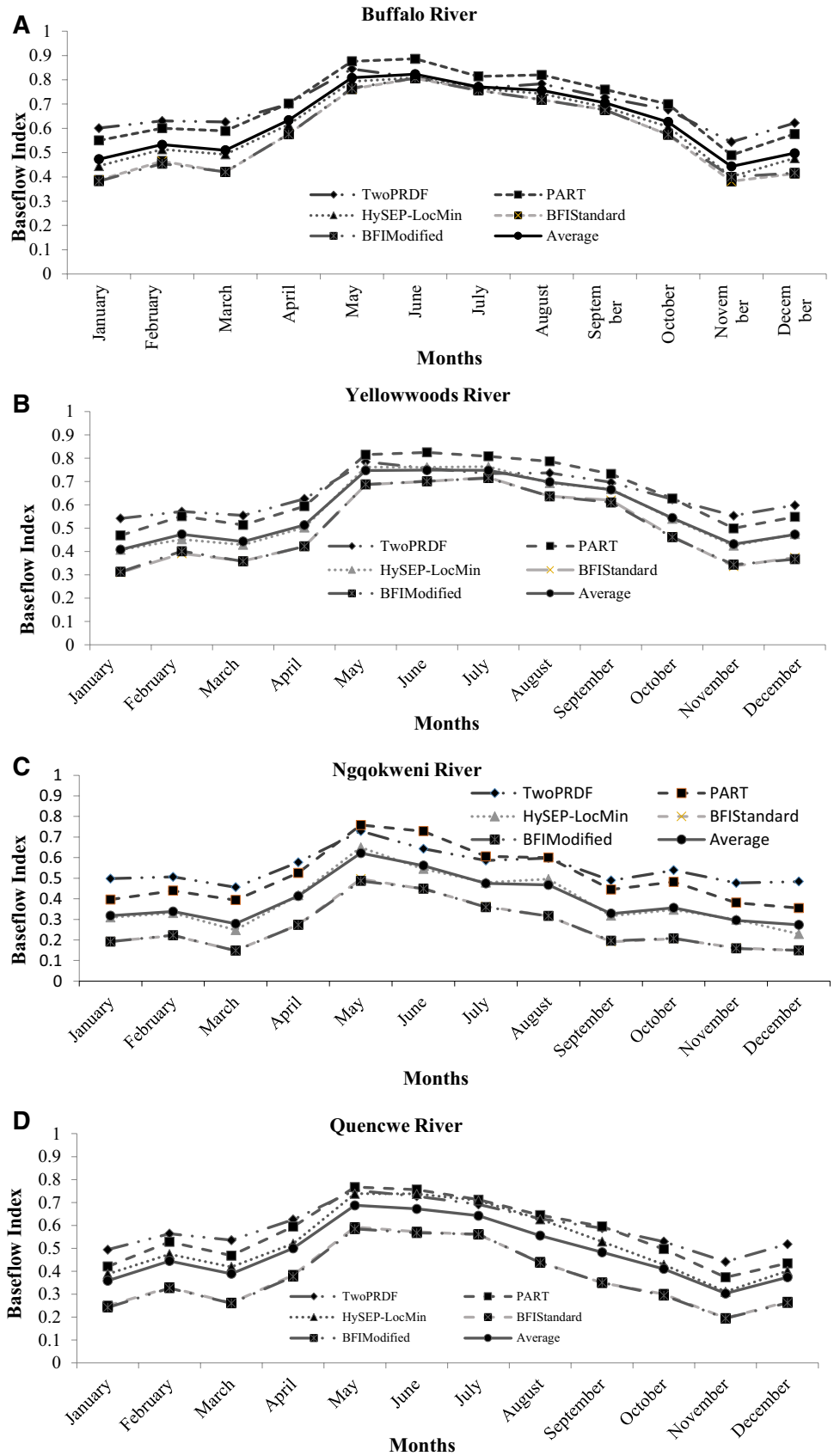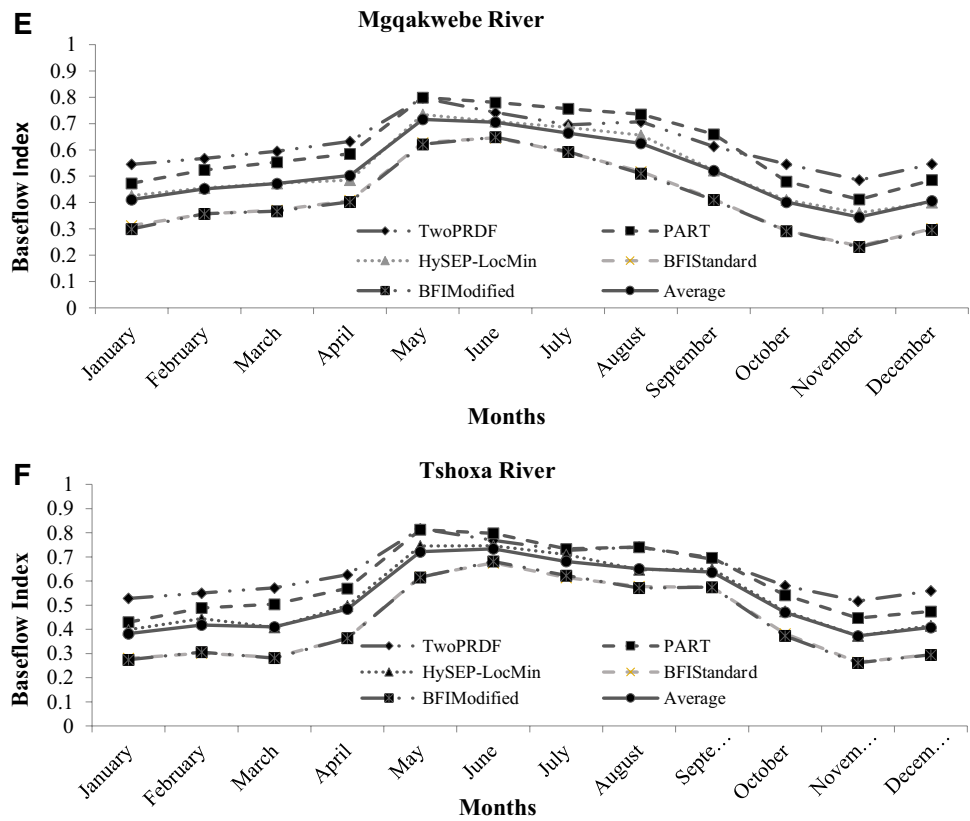
Fig. 5 Analytical signal map showing the areal correlation of high magnetic anomaly with previously mapped dolerite outcrops
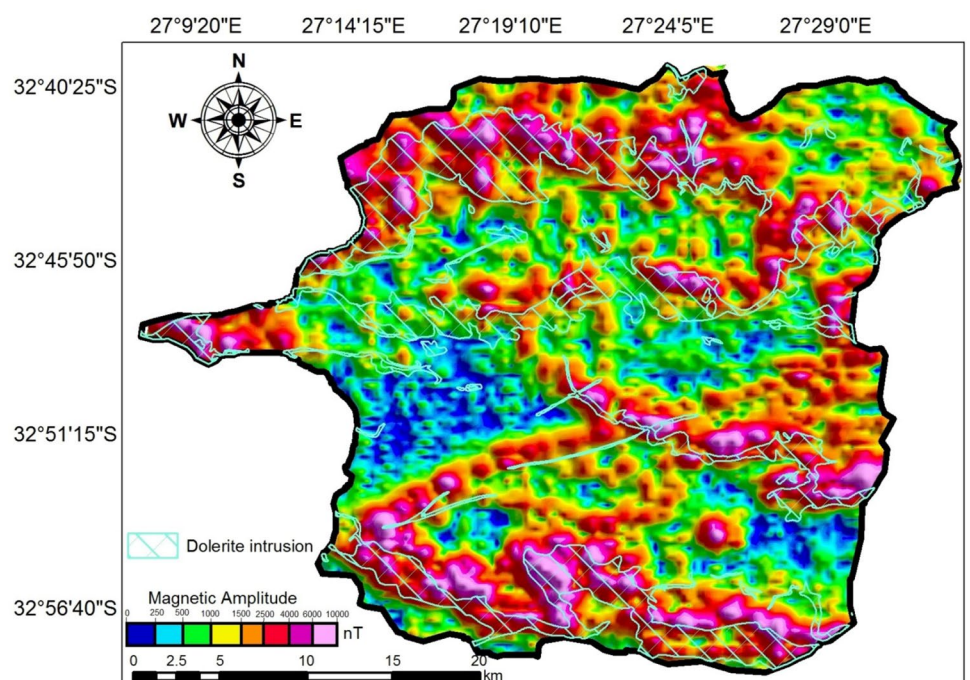
of the favorable hydraulic conductivity of the sandstone which dominated the basin. The Permian–Triassic sandstone of the Tshoxa basin constitutes 40% of surficial lithology. Coarser fractions of the sandstone extend towards the Tshoxa River. The basin is also characterized by the least surficial area of dolerite exposure of about 2%, extending from the East. The high BFI and low-flow in Yellowwoods River indicate that the basin drainage is effectively connected to

Fig. 6 Map showing the distribution of the dominant surficial lithology that may play a major role in the discharge of baseflow in Buffalo catchment
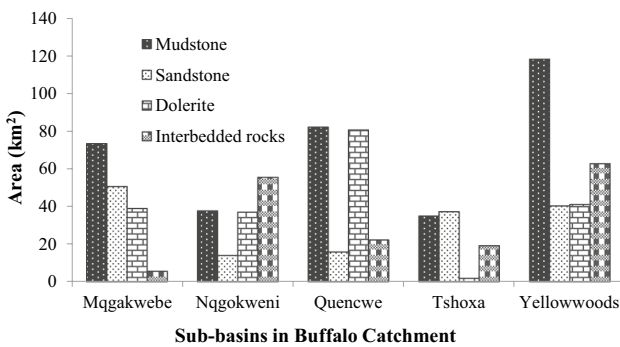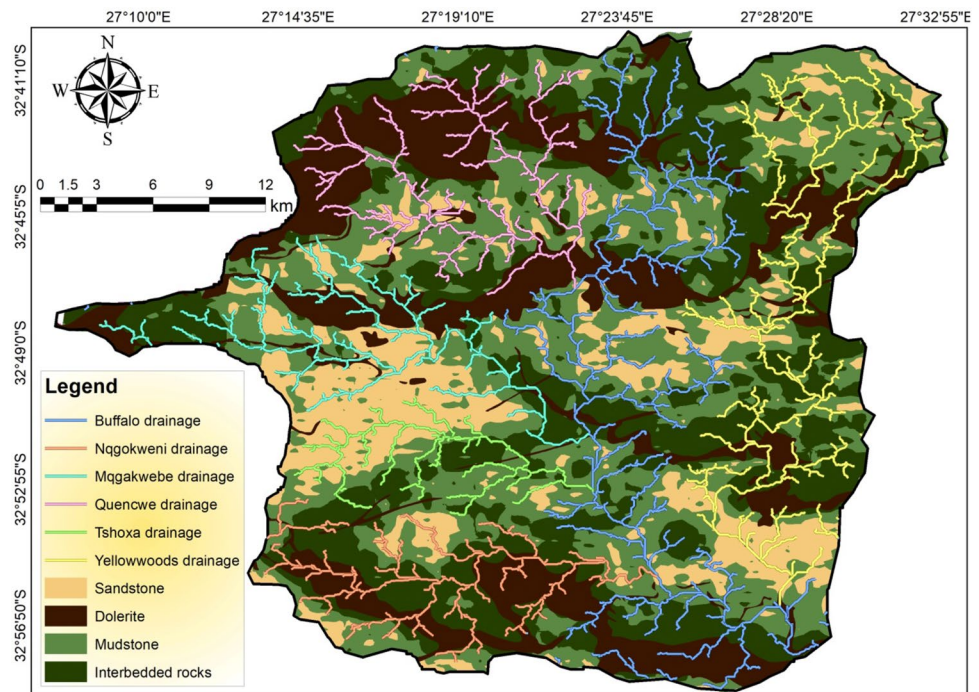
Fig. 7 The plot of the surficial lithology distribution in Buffalo catchment

Buffalo aquifer. The basin is characterized by 45% mudstone, 24% interbedded rock which is chiefly sandy-siltstone and silty-sandstone, 16% weathered and fractured dolerite, and 15% sandstone.

The effective development of the secondary porosity on account of the weathering and fracture system in the dolerite, sandy-siltstone, and mudstone of the basin is possibly the main influence on the baseflow discharge characteristics of the sub-basin. The comparison of lithologic properties of Mgqakwebe and Nqgokweni basins reveals a pattern that suggests the influence of lithologic control on the BFI properties of the basins. Among the three sub-basins, the Mgqakwebe basin has higher sandstone fraction (30%) and lower dolerite fraction (23%), which as a consequence implies the higher potential for connectivity with Buffalo

aquifer. The low-flow and BFI properties of the Quencwe basin are possibly driven by the fracture system and high transmissivity at the contact zone in the sub-basin. Quencwe basin is characterized by the lowest sandstone cover (8%) and with a large dolerite spatial extent (40%), the dolerite is highly fractured and weathered at most of the exposed site. Another important ramification is the possible influence of the hillslope factor on the soil moisture retention at Quencwe basin compared to the Ngqokweni basin. Quencwe basin has a result is characterized by lower solar radiation and possibly lesser evaporative demand due to its abrupt slope and adiabatic property. As a consequence, the Quencwe basin is characterized by canopy tree woodland while the Ngqokweni basin is partly bared-vegetated and veld-related, thus presenting the Quencwe basin as being water-limited while Ngqokweni basin is energy-limited.

Corroboration of recession attributes with borehole yield information

The spatial distribution of the borehole yield across Buffalo watershed is presented in Fig. 9.

Groundwater discharges into rivers through the morphogenetic flow-path, and here, most of the boreholes are at a proximal distance to the drainages. Table 6 and Fig. 9 report the summary of box-and-whisker parameters and plots carried out for the corroboration of streamflow recession analysis.

Fig. 8 Map showing the distribution of borehole water level across Buffalo catchment
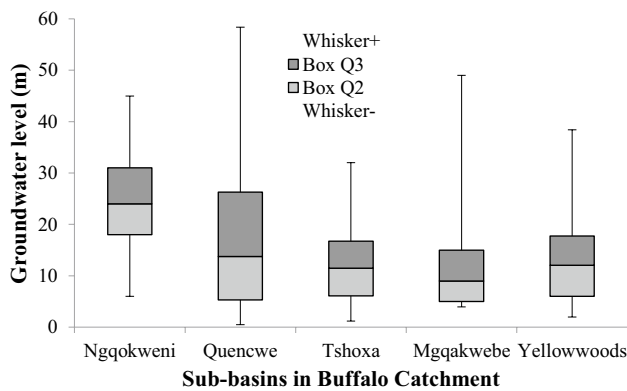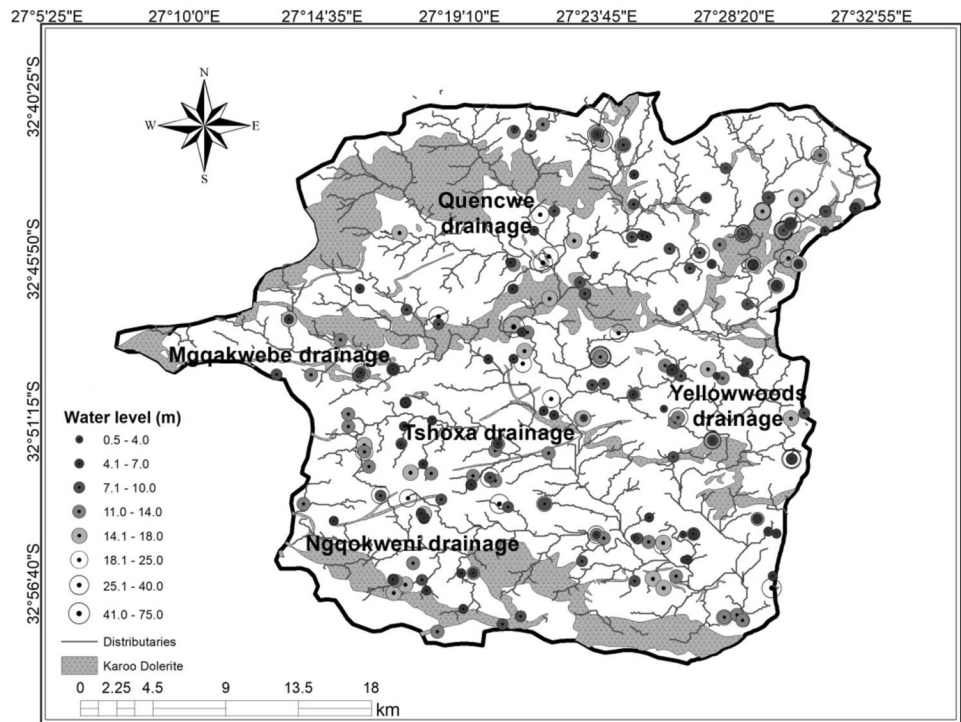
Fig. 9 The box-and-whisker plot of water level across the sub-basins in Buffalo catchment

Table 6 Summary of statistical parameters for box and whisker plots of water level

Parameters	Ngqokweni	Quencwe	Tshoxa	Mgqak-webe	Yel-low-woods
Minimum	6	0.5	1.2	3.96	2
Lower	18	5.32	6.1	5	6.015
Median	24	13.75	11.5	9	12.07
Upper	31	26.2625	16.75	15	17.75
Maximum	45	58.4	32	49	38.4
2Q Box	6	8.43	5.4	4	6.055
3Q Box	7	12.5125	5.25	6	5.68
Whisker-	12	4.82	4.9	1.04	4.015
Whisker+	14	32.1375	15.25	34	20.65

The water level plot reports that the aquifer is shallow at most points of Mgqakwebe, Tshoxa and Yellowwoods basins. These, therefore, confirm the corresponding baseflow discharge and the high BFI in Yellowwoods and Tshoxa stations. The rate of the baseflow discharge is, however, mainly controlled by the geologic structure and the net hydraulic conductivity whereas irrespective of the shallowness of the aquifer. Mgqakwebe station is shown to be the shallowest station meanwhile, it ranks third in baseflow discharge. This suggests that the recharge of Buffalo aquifer mostly occurs at the Mgqakwebe basin while discharge mostly occurs

at the Yellowwoods and Tshoxa. Also, the water level of Quencwe and Ngqokweni basins correspond to their BFI ranking order, thus, suggesting that the streams are often disconnected from the aquifer.

The length of the whisker provides the information on the variability of the water level corresponding to the heterogeneity of the lithostratigraphy. The plot reports that the Quencwe basin is the most heterogeneous while the Tshoxa is the least heterogeneous. Quencwe basin is a hilly terrain, with high relief, and extensive geomorphic dissection, possibly developed from the uplift of the terrain by dolerite

intrusion. The extensive geomorphic dissection of Quencwe drainage may have resulted from a highly frequent hydroclimatic process, heavy downpour, and an accelerated runoff which is ultimately gravitated by the hillslope factor. Ground truthing reveals that the basin is associated with at least three sedimentary facies on account of its steep physiography which may have spread across some Members of the Balfour Formation. Only the Tshoxa basin is possibly associated with sandstone-dominated lithesome of Balfour Formation.

Discussions and implication of streamflow recession and lithology control

The spatial influence of regional atmospheric circulation on precipitation is expected to produce regionally uniform precipitation on a long-term scale or an insignificant variability depending on the influence of relief or proximity to the coast (Ma et al. 2018). On the contrary, the result obtained in this study indicates huge dissimilarities in streamflow response to precipitation, possibly influenced by site-specific factors such as physiography and geology.

The baseflow index (BFI) plots revealed that Buffalo streamflow is perennial, that is, the river is sustained by groundwater discharge from the Buffalo aquifer system. The integration of flows across the drainage channels, especially from the highly drained Yellowwoods and Tshoxa channels favors the sustainability of Buffalo flow. Hence, the catchment mouth can serve as an important capture zone, especially for rainwater harvest. Yellowwoods and Tshoxa streamflow rivers are intermittent and can be said to be well connected to the aquifer system of the catchment. Meanwhile, Mgqakwebe, Quencwe, and Ngqokweni are ephemeral due to the low contribution of baseflow during the dry season.

The broad comparison across streamflow recession assessment and lithology are summarized in Table 7. A comparison of the lithologic properties to the BFI result also reveals some important ramifications about the local geological condition. The high hydraulic conductivity of sandstone as shown in Figs. 7 and 8 which dominates the surficial lithology of the Tshoxa basin explains the high BFI results in the basin. A similar situation can be inferred from the Lithology-BFI comparison of Mgqakwebe station. The smaller area cover of dolerite in the Tshoxa basin also implies that the basin is likely to retain most of its rainfall-induced groundwater recharge. Meanwhile, the potential for such recharge is possibly low in Mgqakwebe basin, probably due to the proportion of the area covered by dolerite outcrop in the sub-basin, and possibly due to low or lack of permissivity zone within Mgqakwebe zone as shown in Fig. 7.

The high BFI of Yellowwoods drainage shows that the river is connected to the fractured aquifer of the catchment. Figure 7 shows that the basin is associated with the highest magnetic amplitude, which also denote the existence of high permissivity zone on account of dolerite-sedimentary rock contact zone. Ground-truthing evidence indicates that the dolerite emplacement in the Northeast of Buffalo catchment was interspersed by weathered siltstone and sandy-siltstone. The intrusion of the sedimentary terrain by dolerite possibly results in the induction of extensional stress which possibly resulted into thermal fracturing and network of lineament arcs within the basin. The water level plot reported in Fig. 10 shows that the porosity network resulting from the geologic structures created in the basin is possibly associated with high hydraulic conductivity. Matter et al. (2006) noted that the intrusion of dolerite is associated with generation of hydrothermal fluid pressure from magma, which cools within its vents and cause thermal contraction and fracturing. The existence of permeable contact zone and its contribution to groundwater discharge in Yellowwoods basin corresponds to Matter et al. (2006) finding.

Table 7 Summary of streamflow recession analysis; FDC and baseflow index results

Period	Low flow slope	Q95	Mean BFI	Lithology %	
				Sandstone	Dolerite
Buffalo	− 0.0113	0.0026	0.541	15	21
Yellowwoods	− 0.0022	0.0008	0.488	15	16
Ngqokweni	− 0.00049	0.0001	0.332	10	26
Quencwe	− 0.0009	0.0002	0.415	8	40
Mgqakwebe	− 0.0017	0.0007	0.443	30	23
Tshoxa	− 0.0029	0.0016	0.450	40	02
Color legend				`	
Color rank	1	2	3	4	5	6

The streamflow recession information of Yellowwoods and Tshoxa drainage show that the contact zone permeability have weightier groundwater discharge influence than net hydraulic conductivity of a lithology system. The long-term impact of interception, evapotranspiration, and evaporation on the wider basin (Yellowwoods drainage) may have possibly resulted in under-estimation of low-flow compared to its baseflow component.

The discrepancy in the streamflow recession results of Quencwe and Ngqokweni stations on account of their lithologic material indicates the overriding influence of local hydro-climatic variation. The high value of skewness and kurtosis produced by long-term streamflow in the Quencwe basin indicates the existence of high hydro-climatic flux in the sub-basin. Quencwe basin has the highest relative relief ratio and this can possibly induce an orographic effect which results in the high hydro-climatic flux. The orographic effect is peculiar to hilly terrain whereby the ascension of the flowing air-mass results in the acceleration of the condensation process in a more frequent manner, rate and intensity compared to the regional trend (Austin and Dirks 2006). Malagó et al. (2018) noted that the inverse power relationship between hillslope length and lateral flow estimation may possibly account for higher residual values for lateral flow where hillslope length is higher. Hence, this finding here aligns with the view of Malagó et al. (2018). Contrarily, the poor streamflow rate in Ngqokweni station may be due to the low hydraulic conductivity of the underlying lithologic material. It is characterized by extreme river diminution whose basin is either detached due to the proportion of area covered by dolerite or famished due to the high proportion of area that is sparsely vegetated in agreement with Vegter and Pitman (2003).

The variability in the performance of the BFI employed in this study conform to the findings of Eckhardt (2005) and Barlow et al. (2015) on calibration variability in metrics of BFI approaches. It is either two-parameter digital filter and PART approaches were overestimated or BFI programs were underestimated. The variation in the estimations can be linked with the unclassified through-flow component of the streamflow. In general, the BFI result is consistent with low-flow assessment to generalize the significance of baseflow during the dry season. The entire results further establish the variability in the performance of watershed, which could be used in determining the exploitation potential of streamflow.

Conclusions

In this study, the spatial variability in streamflow recession is assessed and compared to drainage bedrock properties. The approach is quite unique and different from the previous studies due to the in-depth study of the long-term streamflow recession pattern, the geological characterization of the catchment and the comparative analysis of the two parameters. The following conclusions can be drawn from the study:

- Baseflow information is insufficient for the description of streamflow recession. The spatial inconsistency across the trends of BFI assessment approaches raise the uncertainty on the average BFI estimate. The Q_{95} slope of Stochastic FDC tends to be better and reliable for estimation of environmental flow elasticity.

- Relief variation has a significant impact on the alteration of regional hydro-climatic patterns and streamflow response. The statistical summary and recession analysis indicate the existence of the orographic effect in Quencwe streamflow information and a retrogressive change in the flux of hydro-climatic pattern across the slope. The long-term effect of variation in local atmospheric circulation and hydro-climatic pattern of Quencwe drainage compared to the rest is revealed in the geomorphic dissection and physiographic maturity of the sub-basin.

- In fractured rock hydrastratigraphic regions, permissive contact zone tends to have weightier influence on baseflow discharges than the net hydraulic conductivity of rock types. This is depicted by the fractured mudstone-dominated argillaceous strata of the Yellowwoods basin which produced higher groundwater discharge than the unconsolidated sandstone-dominated arenaceous strata of Tshoxa basin due to the existence of permissive contact zone in sub-basin. Similarly, the Quencwe basin which is dominated by fractured basement rock reported a higher baseflow index than the argillaceous strata of the Ngqokweni basin, on account of existence of permissive contact zone in Quencwe basin.

In general, the flow across Buffalo catchment is perennial. This is possibly due to the favorable hydrogeological productivity of the unconfined fractured aquifer (possibly low–moderate yield) of the watershed which is possibly well connected at Tshoxa and Yellowwoods basins. Further findings indicate that the highly drained rivers in the watershed are associated with the high piezometric head. The recession analyses replicate the heterogeneity of the hydrostratigraphic units in a consistent manner with the topography of the headwater. A conservative action may be required for the prevention of river diminution in the Ngqokweni basin, while Quencwe River indicates the potential for a flash flood. The excellent recession attributes of Buffalo catchment indicate that the catchment mouth can serve as a capture zone for surface water exploitation.

Data statement The dataset used in this study are available in department of water affairs repository (http://www.dwa.gov.za/Hydrology), South Africa. All data generated during this study are included in this work.

Compliance with ethical standards

Conflict of interest The authors declare that there is no conflict of interest, and no human or animal participant involved or harmed in any way during the conduct of this research.

References

Arnold JG, Muttiah RS, Srinivasan R, Allen PM (2000) Regional estimation of base flow and groundwater recharge in the Upper Mississippi river basin. J Hydrol 227(1–4):21–40

Austin GL, Dirks KN (2006) Topographic effects on precipitation. Encyclopedia of hydrological sciences

Bailey GN, Reynolds SC, King GC (2011) Landscapes of human evolution: models and methods of tectonic geomorphology and the reconstruction of hominin landscapes. J Hum Evol 60(3):257–280

Baiyegunhi C (2015) Geological and Geophysical Investigation of the Southeastern Karoo Basin, South Africa (Doctoral dissertation, University of Fort Hare)

Barlow PM, Leake SA (2012) Streamflow depletion by wells: understanding and managing the effects of groundwater pumping on streamflow. US Geological Survey, Reston, p 84

Barlow PM, Cunningham WL, Zhai T, Gray M (2015) U.s. geological survey groundwater toolbox, a graphical and mapping interface for analysis of hydrologic data (version 1.0)—User guide for estimation of base flow, runoff, and groundwater recharge from streamflow data: U.S. Geological Survey Techniques and Methods, book 3, chap B10, p 27

Barros AP, Hodes JL, Arulraj M (2017) Decadal climate variability and the spatial organization of deep hydrological drought. Environ Res Lett 12(10):104005

Barthel R (2014) HESS Opinions "Integration of groundwater and surface water research: an interdisciplinary problem?". Hydrol Earth Syst Sci 18(7):2615–2628

Barthel R, Banzhaf S (2016) Groundwater and surface water interaction at the regional-scale—a review with focus on regional integrated models. Water Resour Manag 30(1):1–32

Basso S, Botter G (2012) Streamflow variability and optimal capacity of run-of-river hydropower plants. Water Resour Res 48:10. https://doi.org/10.1029/2012WR012017

Bates BC, Davies PK (1988) Effect of baseflow separation procedures on surface runoff models. J Hydrol 103(3–4):309–322

Booker DJ, Woods RA (2014) Comparing and combining physically-based and empirically-based approaches for estimating the hydrology of ungauged catchments. J Hydrol 508:227–239

Brierley GJ, Fryirs KA (2013) Geomorphology and river management: applications of the river styles framework. Wiley, Oxford

Burgan HI, Aksoy H (2018) Annual flow duration curve model for ungauged basins. Hydrol Res 49(5):1684–1695

Burgan HI, Aksoy H (2020) Monthly flow duration curve model for ungauged river basins. Water 12:338

Burn DH, Elnur MAH (2002) Detection of hydrologic trends and variability. J Hydrol 255(1–4):107–122

Carlier C, Wirth SB, Cochand F, Hunkeler D, Brunner P (2018) Geology controls streamflow dynamics. J Hydrol 566:756–769

Castellarin A, Galeati G, Brandimarte L, Montanari A, Brath A (2004) Regional flowduration curves: reliability for ungauged basins. Adv Water Resour 27:953–965

Catuneanu O, Elango HN (2001) Tectonic control on fluvial styles: the Balfour Formation of the Karoo Basinm, South Africa. Sedim Geol 140(3–4):291–313

Chapman T (1999) A comparison of algorithms for stream flow recession and baseflow separation. Hydrol Process 13(5):701–714

Cimen M, Saplioglu K (2004,) A procedure for separation of baseflow. In: Conference of water observation and information system for decision support (BALWOIS), pp 25–29

Collischonn W, Fan FM (2013) Defining parameters for Eckhardt's digital baseflow filter. Hydrol Process 27(18):2614–2622

Croker KM, Young AR, Zaidman MD, Rees HG (2003) Flow duration curve estimation in ephemeral catchments in Portugal. Hydrol Sci J 48(3):427–439

Eckhardt K (2005) How to construct recursive digital filters for baseflow separation. Hydrol Processes Int J 19(2):507–515

Esralew RA, Lewis JM (2010. Trends in base flow, total flow, and base-flow index of selected streams in and near Oklahoma through 2008 (No. 2010-5104). US Geological Survey

Fennessey N, Vogel RM (1990) Regional flow-duration curves for ungauged sites in Massachusetts. J Water Resour Plann Manage 116(4):530–549

Gore JA, Banning J (2017) Discharge measurements and streamflow analysis. Methods in stream ecology, vol 1. Academic Press, New York, pp 49–70

Gustard A, Demuth S (2009) Manual on low-flow estimation and prediction. http://ihp.bafg.de

Haaf E, Barthel R (2018) An inter-comparison of similarity-based methods for organisation and classification of groundwater hydrographs. J Hydrol 559:222–237

Hamel P, Fletcher TD (2014) Modelling the impact of stormwater source control infiltration techniques on catchment baseflow. Hydrol Process 28(24):5817–5831

Institute of Hydrology (Great Britain) (1980) Low flow studies reports. Institute of Hydrology

Jha R, Sharma KD, Singh VP (2008) Critical appraisal of methods for the assessment of environmental flows and their application in two river systems of India. KSCE J Civ Eng 12(3):213–219

Johnson MR (1976) Stratigraphy and sedimentology of the Cape and Karoo sequences in the Eastern Cape Province

Johnson MR, Van Vuuren CJ, Visser JNJ, Cole DI, Wickens HDV, Christie ADM, Roberts DL, Brandl G (2006) Sedimentary rocks of the Karoo Supergroup. Geol South Afr 20:461–499

Kienzle SW (2006) The use of the recession index as an indicator for streamflow recovery after a multi-year drought. Water Resour Manag 20(6):991–1006

Krzywinski M, Altman N (2014) Points of significance: visualizing samples with box plots

Le Maitre DC, Colvin CA (2008) Assessment of the contribution of groundwater discharges to rivers using monthly flow statistics and flow seasonality. Water SA 34(5):549–564

Liu S, Hu X, Zhang H, Geng M, Zuo B (2017) 3D magnetization vector inverion of magnetic data: improving and comparing methods. Pure Appl Geophys 174(12):4421–4444

Longobardi A, Van Loon AF (2018) Assessing baseflow index vulnerability to variation in dry spell length for a range of catchment and climate properties. Hydrol Process 32(16):2496–2509

Lott DA, Stewart MT (2013) A power function method for estimating base flow. Groundwater 51(3):442–451

Ma J, Chadwick R, Seo KH, Dong C, Huang G, Foltz GR, Jiang JH (2018) Responses of the tropical atmospheric circulation to climate change and connection to the hydrological cycle. Annu Rev Earth Planet Sci 46:549–580

Mair A, Fares A (2011) Time series analysis of daily rainfall and streamflow in a volcanic dike-intruded aquifer system, O 'ahu, Hawai 'i, USA. Hydrogeol J 19(4):929–944

Malagó A, Vigiak O, Bouraoui F, Pagliero L, Franchini M (2018) The hillslope Length impact on SWAT streamflow prediction in large Basins. J Environ Inform 32(2):82–97

Matter JM, Goldberg DS, Morin RH, Stute M (2006) Contact zone permeability at intrusion boundaries: new results from hydraulic testing and geophysical logging in the Newark Basin, New York, USA. Hydrogeol J 14:689–699

Mayer TD, Naman SW (2011) Streamflow response to climate as influenced by geology and elevation. J Am Water Resour Assoc 47(4):724–738

Mirus BB, Loague K (2013) How runoff begins (and ends): characterizing hydrologic response at the catchment scale. Water Resour Res 49(5):2987–3006

Müller MF, Dralle DN, Thompson SE (2014) Analytical model for flow duration curves in seasonally dry climates. Water Resour Res 50(7):5510–5531

Naef F, Margreth M, Floriancic M (2015) Festlegung von Restwassermengen: Q347, eine entscheidende, aber schwer zu fassende Größe. Wasser Energie Luft Heft 4(107. Jahrgang):277–284

Nippgen F, McGlynn BL, Marshall LA, Emanuel RE (2011) Landscape structure and climate influences on hydrologic response. Water Resour Res 47(12):1–17

Oghenekome ME, Chatterjee TK, Hammond NQ, van Bever Donker JM (2016) Provenance study from petrography of the late Permian-Early Triassic sandstones of the Balfour Formation Karoo Supergroup, South Africa. J Afr Earth Sci 114:125–132

Peddie NW (1982) International geomagnetic reference field. J Geomagn Geoelectr 34(6):309–326

Pettyjohn WA, Henning RJ (1979) Preliminary estimate of regional effective ground-water recharge rates in Ohio. Ohio State University, Water Resources Center, Ohio

Pfister L, Martínez-Carreras N, Hissler C, Klaus J, Carrer GE, Stewart MK, McDonnell JJ (2017) Bedrock geology controls on catchment storage, mixing, and release: a comparative analysis of 16 nested catchments. Hydrol Process 31(10):1828–1845

Price K (2011) Effects of watershed topography, soils, land use, and climate on baseflow hydrology in humid regions: a review. Prog Phys Geogr 35(4):465–492

Requena AI, Chebana F, Ouarda TB (2018) A functional framework for flow-duration-curve and daily streamflow estimation at ungauged sites. Adv Water Resour 113:328–340

Rivers-Moore NA, De Moor FC, Morris C, O'keeffe J (2007) Effect of flow variability modification and hydraulics on invertebrate communities in the Great Fish River (Eastern Cape Province, South Africa), with particular reference to critical hydraulic thresholds limiting larval densities of Simulium chutteri Lewis (Diptera, Simuliidae). River Res Appl 23(2):201–222

Rudra RP, Ahmed SI, Khayer M, Dickinson WT, Gharabaghi B (2010) the relationship between watershed physiography, tile flow, and streamflow characteristics. In: 9th international drainage symposium held jointly with CIGR and CSBE/SCGAB proceedings, 13–16 June 2010, Québec City Convention Centre, Quebec City, Canada. American Society of Agricultural and Biological Engineers, p 1

Rutledge AT (1998) Computer programs for describing the recession of ground-water discharge and for estimating mean ground-water recharge and discharge from streamflow records: update (No. 98). US Department of the Interior, US Geological Survey

Sanz DB, Atienzar IP (2018) A new method for environmental flow assessment based on basin geology: application to the Ebro Basin. Water Environ Resour 90:826

Sarailidis G, Vasiliades L, Loukas A (2019) Analysis of streamflow droughts using fixed and variable thresholds. Hydrol Process 33(3):414–431

Searcy JK (1959) Flow-duration curves. US Government Printing Office

Slaughter AR, Mantel SK, Hughes DA (2014) Investigating possible climate change and development effects on water quality within an arid catchment in South Africa: a comparison of two models

Smakhtin VU (2001) Low flow hydrology: a review. Hydrology 240(3–4):147–186

Stewart MK, Morgenstern U, McDonnell JJ (2010) Truncation of stream residence time: how the use of stable isotopes has skewed our concept of streamwater age and origin. Hydrol Process 24(12):1646–1659

Stuckey MH (2006) Low-flow, base-flow, and mean-flow regression equations for Pennsylvania streams. U. S. Geological Survey, New York

Van Wyk E, Van Tonder GJ, Vermeulen D (2012) Characteristics of local groundwater recharge cycles in South African semi-arid hard rock terrains: rainfall–groundwater interaction. Water SA 38(5):747–754

Vegter JR, Pitman WV (2003) Recharge and stream flow. In: Xu Y, Beekman E (eds) Groundwater recharge estimation in southern Africa. UNESCO IHP Series, vol 64. UNESCO, Paris, pp 109–123

Verma RK, Murthy S, Verma S, Mishra SK (2017) Design flow duration curves for environmental flows estimation in Damodar River Basin, India. Appl Water Sci 7(3):1283–1293

Vogel RM, Kroll CN (1992) Regional geohydrologic-geomorphic relationships for the estimation of low-flow statistics. Water Resour Res 28(9):2451–2458

Wahl KL, Wahl TL (1995) Effects of regional ground-water declines on streamflows in the Oklahoma Panhandle. In: Symposium on water-use data for water resources management, AWRA, Tucson, Arizona, pp 239–249

Ward RC, Robinson M (1990) Principles of hydrology. McGraw-Hill, Maidenhead

Wella-Hewage CS, Alankarage Hewa G, Pezzaniti D (2015) Can water sensitive urban design systems help to preserve natural channel-forming flow regimes in an urbanized catchment? Water Sci Technol 73(1):78–87

Wilson A, Flint S, Payenberg T, Tohver E, Lanci L (2014) Architectural styles and sedimentology of the fluvial lower Beaufort Group, Karoo Basin, South Africa. Sedim Res 84(4):326–348

Wittenberg H (1999) Baseflow recession and recharge as nonlinear storage processes. Hydrol Process 13(5):715–726

Xu Y, Titus R, Holness SD, Zhang J, van Tonder GJ (2002) A hydrogeomorphological approach to quantification of groundwater discharge to streams in South Africa. Water SA 28(4):375–380

Ye L, Ding W, Zeng X, Xin Z, Wu J, Zhang C (2018) Inherent relationship between flow duration curves at different time scales: a perspective on monthly flow data utilization in daily flow duration curve estimation. Water 10(8):1008

Zhang Y, Singh V, Byrd A (2017) Entropy parameter M in modeling a flow duration curve. Entropy 19(12):654